

In Vivo Detection of Single Cells by MRI

Erik M. Shapiro,* Kathryn Sharer, Stanko Skrtic, and Alan P. Koretsky

The use of high-relaxivity, intracellular contrast agents has enabled MRI monitoring of cell migration through and homing to various tissues, such as brain, spinal cord, heart, and muscle. Here it is shown that MRI can detect single cells in vivo, homing to tissue, following cell labeling and transplantation. Primary mouse hepatocytes were double-labeled with green fluorescent 1.63- μm iron oxide particles and red fluorescent endosomal labeling dye, and injected into the spleens of recipient mice. This is a common hepatocyte transplantation paradigm in rodents whereby hepatocytes migrate from the spleen to the liver as single cells. One month later the animals underwent in vivo MRI and punctuated, dark contrast regions were detected scattered through the livers. MRI of perfused, fixed samples and labeled hepatocyte phantoms in combination with histological evaluation confirmed the presence of dispersed single hepatocytes grafted into the livers. Appropriate controls were used to determine whether the observed contrast could have been due to dead cells or free particles, and the results confirmed that the contrast was due to disperse, single cells. Detecting single cells in vivo opens the door to a number of experiments, such as monitoring rare cellular events, assessing the kinetics of stem cell homing, and achieving early detection of metastases. Magn Reson Med 55:242–249, 2006. Published 2006 Wiley-Liss, Inc.†

Key words: MRI; iron oxide; cells; contrast agents; liver

Noninvasive imaging of single cells in intact, live organisms would have an enormous impact in all fields involved in cell transplantation, early detection of cell homing, and monitoring cell migration. There is growing interest in using MRI to track cells after they are labeled with iron oxide contrast agents. Some specific applications include stem cell tracking to damaged myocardium (1), early detection of tissue rejection (2), early detection of cancer (3), and tracking neural stem cell response to stroke (4). To date, single cells have been imaged in vitro in culture using MRI (5–8). This method was recently extended to visualizing single cells and single particles in in vitro embryo samples by MRI (7).

Since the first example of “immunospecific NMR agents” was reported in 1986 by Renshaw et al. (9), there has been increasing emphasis on both improving the detection instrumentation of MRI and augmenting the relaxivities and delivery of reporter contrast agents, with one goal being in vivo

single cell detection. Improvements in gradient coil design and higher field magnets have enabled image resolution to approach 50 μm in live animals. Cell labeling contrast agents are primarily composed of iron oxide or gadolinium in the form of coated particles, dendrimer-based structures, or simple chelates. Strategies for cellular uptake of contrast agents in culture include the use of micron-sized particles (6,10), transfection agents (11), receptor-mediated delivery (12), antibody-mediated delivery (13), combined receptor/antibody-mediated delivery (14), and conjugated cellular translocation signal peptides (15). In vivo cell labeling is currently limited to macrophages (2), and some initial reports have described in vivo labeling of peripheral T cells (16) and neural stem cells (17).

In this study we used a well developed model for liver cell transplantation to demonstrate that single-cell detection in vivo can be achieved with MRI. Given the scarcity of donor livers, one proposed method for gene therapy within the liver, or to repair damaged liver, is to administer donor hepatocytes to patients (18). Cells can be administered via several routes, with the preferred route in rodents being an intersplenic injection (19). This is also the preferred route for clinical treatment when extensive tissue damage is present in the liver. Cells can then migrate out of the spleen to the liver, where they engraft. Not all cells migrate to the liver, however; some go to the lungs, some engraft in the spleen, and others die. The important fact is that they migrate and engraft as single cells (20).

Primary mouse hepatocytes were labeled with both superparamagnetic and fluorescent agents, and transplanted into the spleens of recipient mice. Micron sized iron oxide particles (MPIOs; 1.63 μm in diameter) were used as the superparamagnetic label. Previous reports demonstrated that these particles are efficiently endocytosed by a wide variety of cell types, with labeling capacity as high as hundreds of picograms of iron per cell, and cell viability of 95% (10,17). One month after transplantation the animals underwent MRI investigations, and their tissues were subsequently harvested for histological analysis. The results indicate that single cells can be detected in the liver. Furthermore, possible artifacts due to dead cells or free particles are considered and approaches for separating these from hepatocyte engraftment are described.

MATERIALS AND METHODS

Cell Isolation, Labeling, and Imaging

Mouse hepatocytes were isolated from female C57Bl/6 mice by the collagenase perfusion method, followed by repeated centrifugations according to Seglen (21). Isolated hepatocytes were suspended and cultured in Dulbecco's modified Eagle's medium/Hams's F-12 (GIBCO, Gaithers-

Laboratory of Functional and Molecular Imaging, National Institute of Neurological Disorders and Stroke, National Institutes of Health, Bethesda, Maryland, USA.

*Correspondence to: Erik M. Shapiro, Laboratory of Functional and Molecular Imaging, National Institute of Neurological Disorders and Stroke, National Institutes of Health, Bethesda, MD 20892. E-mail: ShapiroE@ninds.nih.gov
Received 16 December 2004; revised 11 July 2005; accepted 10 August 2005.

2005 ISMRM Young Investigator W.S. Moore Award Finalist
DOI 10.1002/mrm.20718

Published online 13 January 2006 in Wiley InterScience (www.interscience.wiley.com).

Published 2006 Wiley-Liss, Inc. † This article is a US Government work and, as such, is in the public domain in the United States of America.

burg, MD, USA) with 5% fetal bovine serum, 2 mM glutamine, 0.875 μ M bovine insulin, 100 nM dexamethasone, 5 ng/ml epidermal growth factor, 100 U/ml penicillin, and 100 μ g/ml streptomycin. Cells were plated at a density of 1×10^6 cells/cm² on plastic culture flasks (TissueCulture, Greiner, Longwood, FL) and allowed to attach. To magnetically label the cells, 3×10^8 1.63- μ m-diameter, COOH functionalized, polystyrene/divinyl benzene-coated MPIOs (Bangs Laboratories, Fishers, IN, USA) in 100 μ l growth medium were added directly to the culture flask and incubated with the cells for 18 hr.

To remove free particles after labeling, the cells were first washed extensively to remove loosely bound free particles. They were then released from the dish by incubation with trypsin. To remove additional free MPIOs, the cells were pelleted, and resuspended in growth medium at 10^6 /ml, and density centrifugation through Ficoll-Paque PLUS (Amersham Biosciences, Piscataway, NJ, USA) was performed. Briefly, 3 ml of Ficoll-Paque PLUS was added to 15-ml plastic Falcon tubes. Then 3 ml of resuspended cells were layered on top of the Ficoll-Paque PLUS, with care taken to not disturb the interface. The tubes were centrifuged for 30 min at $400 \times g$. After centrifugation, most free particles had pelleted to the bottom of the tube, and the cells remained at the interface of the Ficoll-Paque PLUS and growth medium. The cells were removed with a glass pipette and washed with growth medium to remove trace Ficoll-Paque PLUS. At this point, the cells were also labeled with a red fluorescent cell tracker dye (CM-DII; Molecular Probes, Eugene, OR, USA) according to the manufacturer's directions. This consisted of a 15-min incubation of cells in suspension at 37°C with the cell tracker dye, followed by a 15-min incubation in ice. The cells were then washed twice to remove free dye. Cell death was measured via Trypan blue exclusion tests at each labeling step. For the hepatocyte phantom, 10^4 labeled cells were embedded in 1 ml 1% agarose made with 1 mM Gd-DTPA (Magnevist, Berlex Labs, Wayne, NJ, USA) to shorten the T_1 to allow rapid MRI.

T_2^* -weighted 3D gradient-echo imaging of the hepatocyte phantom was performed at 7.0 T on a Bruker Biospec MRI system (Bruker BioSpin, Billerica, MA, USA). Images were acquired at two different resolutions: $100 \times 100 \times 100$ and $100 \times 100 \times 300$ μ m. Other imaging parameters were TR = 100 ms, TE = 4 ms, and FOV = $2.56 \times 2.56 \times 1.28$ cm. A 35-mm birdcage coil was used. The size of the susceptibility-induced signal decrease caused by the cells loaded with MPIOs was measured in both data sets using programs written in Interactive Data Language (Research Systems Inc., Boulder, CO, USA). Images were thresholded at the noise level, and the size of seven random hypointense areas was measured by summing pixels.

Hepatocyte Transplantation and Imaging

C57Bl/6 mice (males and females, 3 months old) were used as both hepatocyte donors and transplant recipients. Each recipient mouse was anesthetized by isoflurane inhalation. The abdomen was incised at the site of the spleen, and the spleen was partly pushed out. Then 100 μ l of hepatocyte suspension (10^6 cells, +4C) were injected in the tip of the spleen ($N = 12$ animals). The spleen was gently pushed

back in the abdomen and the incision was closed. The mice were also injected with free particles ($N = 6$), heat-killed labeled cells ($N = 3$), and labeled mouse embryonic fibroblasts ($N = 3$). For the free-particle injection, 3×10^7 particles (equivalent to 30 particles per injected cell) were used. One mouse received 3×10^7 particles via tail vein injection, with imaging performed within 30 min. This corresponds to 1.5 times more iron than the standard clinical dose of Feridex. Some mice ($N = 3$) received no injection at all.

At 1 month posttransplantation, the mice underwent MRI examinations. The MRI parameters used were based on a previous study that outlined MRI guidelines for single-cell detection of labeled cells, including imaging parameters and minimum voxel sizes (10,17). T_2^* -weighted multislice gradient-echo imaging was performed using a 72-mm transmit volume coil in conjunction with a 35-mm surface receive-only coil. The animals were placed supine on the surface coil, with a respiratory gating balloon (SA Instruments, Inc., Stony Brook, NY, USA) placed over the lower chest. Coronal and axial images were acquired at $100 \times 100 \times 300$ μ m resolution. Other imaging parameters were TR = 100 ms, TE = 4 ms, FOV = 4.00×4.00 cm, flip angle = 30°, four to six slices, and respiratory gating. MRI, including the periodic pauses in the sequence due to the respiratory gating, took on average 30 min. Typical signal-to-noise ratios (SNRs) were 30–50. The mice were then perfused and fixed with 4% formaldehyde, and the livers were removed and placed in saline. 3D gradient-echo MRI was performed (TE = 4 ms, TR = 100 ms) at 100 μ m isotropic resolution. The livers and spleens were then sectioned for histology at 10 μ m thickness (HistoServe, Germantown, MD). The sections were either stained for iron with Prussian blue staining or left unstained. Fluorescence stereomicroscopy was used to obtain wide-field views of unstained liver sections and analyze the separation between labeled cells. Confocal microscopy (Zeiss LSM 510; Carl Zeiss, Thronwood, NY, USA) was used to identify transplanted cells by observing both the fluorescent green MPIOs and the red cell tracker dye on unstained sections. The area encompassed by the dark contrast spots in the livers was calculated in the same manner used for the cell phantom.

RESULTS

The extent of hepatocyte intracellular labeling by the 1.63- μ m MPIOs and the fluorescent cell tracker probe is shown in Fig. 1. Figure 1a shows a stereomicroscope image of a labeled cell. The particles were dark and surrounded the nuclei of the hepatocyte. This labeling pattern was observed for nearly every cell in every batch labeled. Figure 1b shows a confocal fluorescent image displaying both green fluorescence from the particles and red fluorescence from the cell tracker. Again, the particles can be seen surrounding the nuclei of this hepatocyte. Interestingly, the particles appear to be in different endosomes than the red cell tracker dye, likely because the two labeling schemes occurred at different times. More than 50 particles could be counted in most cells. Since each particle contains ~ 1.1 pg of iron, the cells were labeled with >50 pg of iron, consistent with previous reports of cellular labeling of hepatocytes with 1.63- μ m MPIOs (10). Greater

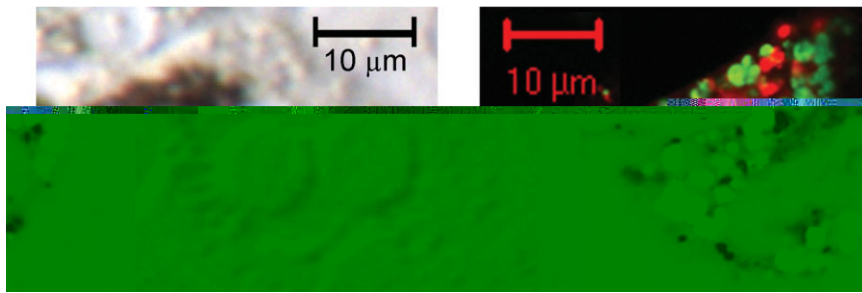


FIG. 1. **a:** Bright-field microscopic image of a single hepatocyte labeled with 1.63- μm MPIOs. **b:** Dual-channel confocal fluorescence microscopic image of a different cell, showing >50 green fluorescent MPIOs and red fluorescence from the cell tracker.

than 90% of cells contained particles, with cell survival greater than 95% following the overnight incubation with the particles. Cell viability following cell tracker labeling was almost 100%.

Figure 2 shows coronal MRI slices of the livers of animals that received live double-labeled hepatocytes. Figure 2a shows the liver from a control animal that did not undergo any procedure prior to imaging. Due to the rapid TR, the blood signal appears bright and vessels are clearly visible. The tissue is homogeneous in signal intensity at this resolution and imaging conditions. Also visible are the kidneys and the space occupied by the lungs. The heart appears as a fuzzy oval shape because cardiac gating was not employed. Figure 2b shows data from a mouse that received an intersplenic injection of 10^6 live, double-labeled cells in 100 μl PBS. Punctuated dark contrast spots were distributed fairly uniformly in the liver in both the coronal and the axial directions (data not shown). In all, nine of 12 animals injected displayed dark, punctuated contrast in the livers. While most of these animals ($N = 7$, Fig. 2b and f) demonstrated dark contrast spots dispersed uniformly throughout the liver, some did not ($N = 2$, Fig. 2e). The spacing between dark contrast spots ranged from 100 μ to several millimeters.

Figure 2c and d show in vitro coronal MRI slices of a single perfused and fixed liver lobe from the same control and experimental animals shown in Fig. 2a and b. These high-resolution images help to identify the distribution of the contrast in the liver, free from motion artifacts and blood. The contrast between the livers and the saline was set equal to ensure that observed contrast was not due to saline in the vessels of the liver. The control liver in Fig. 2c was completely uniform in signal intensity. Figure 2d shows the liver from the animal that received live labeled cells. As expected, dark contrast regions were dotted throughout the liver lobe, with very little underlying graininess.

Figure 3a–d shows representative histological analyses for the animals that received live labeled cells. Figure 3a displays a wide-field, stereomicroscope image showing the green fluorescence from the Bangs particles. Two general size clusters are visible: 1) single, dispersed green particles, and 2) compact groups of particles. The compact groups of particles are circled and the distances between them are indicated in microns. In this field the distances ranged from 387 to 680 μm , but distances as short as 100 μm and as long as millimeters were observed in other sections. Figure 3b shows a portion of a histological section stained with Prussian blue for iron. Readily visible is

FIG. 2. In vivo MRI slice of (a) a control liver and (b) a liver from an animal whose spleen was injected with labeled hepatocytes 1 month prior to imaging. c and d: In vitro MRI slices of the same samples shown in a and b. The dotted outline in c delineates the liver boundary. e and f: In vivo MRI slices from two other animals that received live labeled hepatocytes. Scale bars are in centimeters.

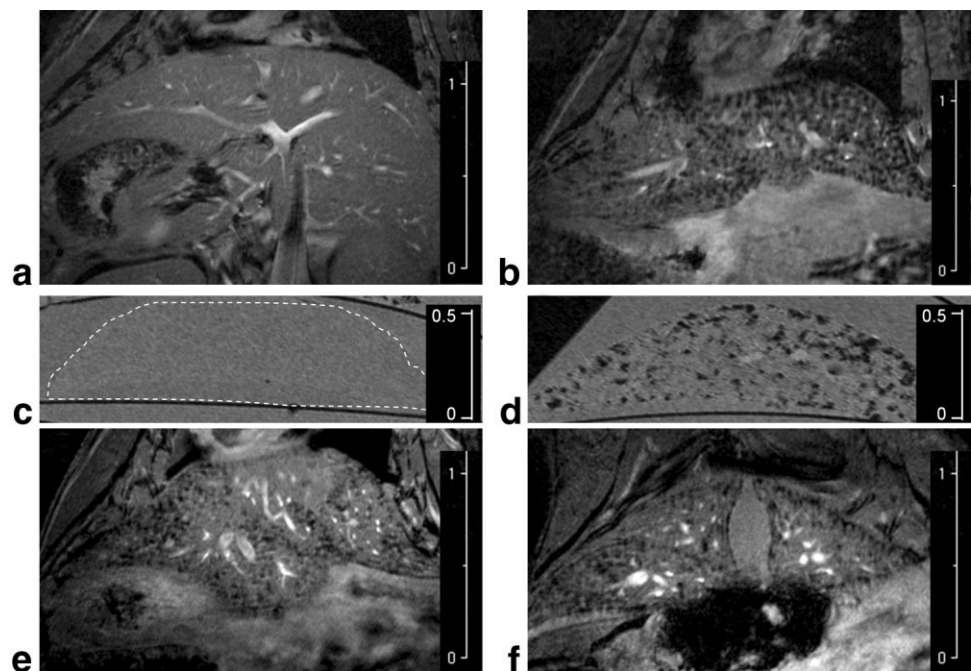
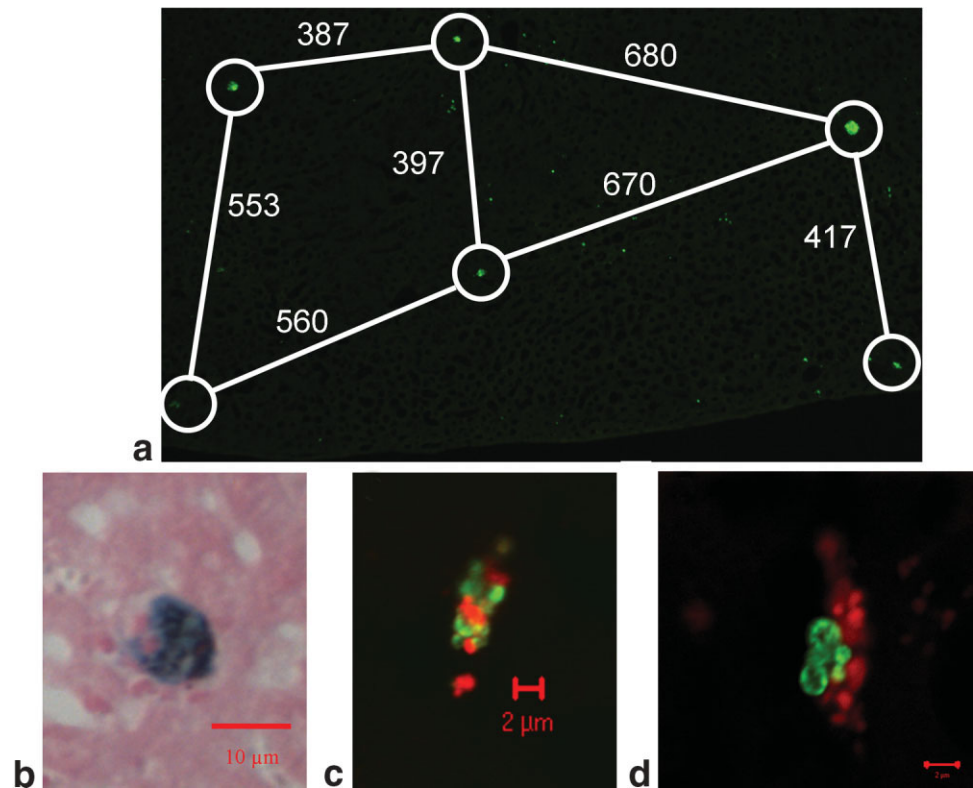


FIG. 3. Microscopic images of histological sections from intersplenic labeled hepatocyte injection. **a:** Wide-field green fluorescent stereomicroscopic image of a liver section showing intact groups of particles (circled). Distances between cells are given in microns. **b:** Prussian blue-stained cell showing particles surrounding the nucleus of a grafted cell in the liver. **c** and **d:** Two dual-channel confocal fluorescence images of grafted hepatocytes in the liver showing green MPIOs and red cell tracker dye.



the dark blue staining that is indicative of iron, surrounding the nuclei of a hepatocyte. This distribution of particles within the cell is similar to the pattern observed in the cells pretransplantation. Figure 3c shows a portion of a confocal microscope image displaying a hepatocyte in the liver with colocalized green fluorescent particles and red fluorescent endosomes. Figure 3d shows a view of a different hepatocyte, again with colocalized green particles and red endosomes.

Control experiments were performed to determine what would happen to the particles (and hence contrast in the liver) if the transplanted cells died. Figure 4a shows an MR image from an animal that received the same number of heat-killed cells transplanted into the spleens. Significant differences were observed in the contrast in the liver. Instead of being punctuated, the contrast was grainy and less intense. Additionally, the contrast was organized in dark, circular structures apparent throughout the liver lobes. In vitro MRI (Fig. 4b) shows a liver in which the signal intensity appears very grainy with very few scattered dark contrast regions, as can be seen in the liver in Fig. 2b and d. The circular structures also became more clearly visualized. Fluorescence stereomicroscopy detected scattered single particles within the liver, with no major groupings of particles (Fig. 4i and j). Confocal fluorescence microscopy detected no cells with colocalized red and green fluorescence.

To test whether free particles could travel from the spleen to the liver, and what kind of contrast that would elicit, the same number of free particles injected with the labeled cells were injected into the spleen. Figure 4c shows a liver from this set of experiments. The particles indeed reached the liver, but the contrast in the liver was markedly different, being more grainy and again forming

circular structures. The dark punctuated spots observed in Fig. 2b are not present. Figure 4d shows the in vitro MR image of the liver from the same animal. Here the graininess, organized into circular structures, can best be seen. Fluorescence stereomicroscopy showed only scattered particles throughout the liver (Fig. 4k and l).

A second experiment with free particles involved an injection of the same number of particles, this time intravenously. This served to label Kupffer cells in the liver directly and delineate which cells likely received the particles in the previous experiment. Figure 4e shows the liver from this experiment. Here, because the spleen was bypassed, particles could go directly to the liver and the contrast was darker and more widespread. Again, the contrast was grainy and formed circular structures. Figure 4f shows the in vitro MR image from the liver of this animal. The grainy contrast is more intense than that in Fig. 4d, as in the in vivo images, but is still organized into circular structures. Fluorescence stereomicroscopy again detected many scattered, single particles without detecting any scattered groups of clustered particles (data not shown).

As a final control, labeled mouse embryonic fibroblasts were injected into the spleens. These cells were not expected to undergo major migration to the liver. Figure 4g shows the liver of one animal that received the same number of labeled fibroblasts as were delivered with hepatocytes. No punctuated dark contrast regions were observed in the liver, and there was only some slight graininess, as was observed in the two previous examples. Figure 4h shows the in vitro MR image of the liver from this animal. Mild graininess was observed, with a very few scattered dark contrast regions similar in size to the contrast regions observed in Fig. 2b. Fluorescence stereomi-

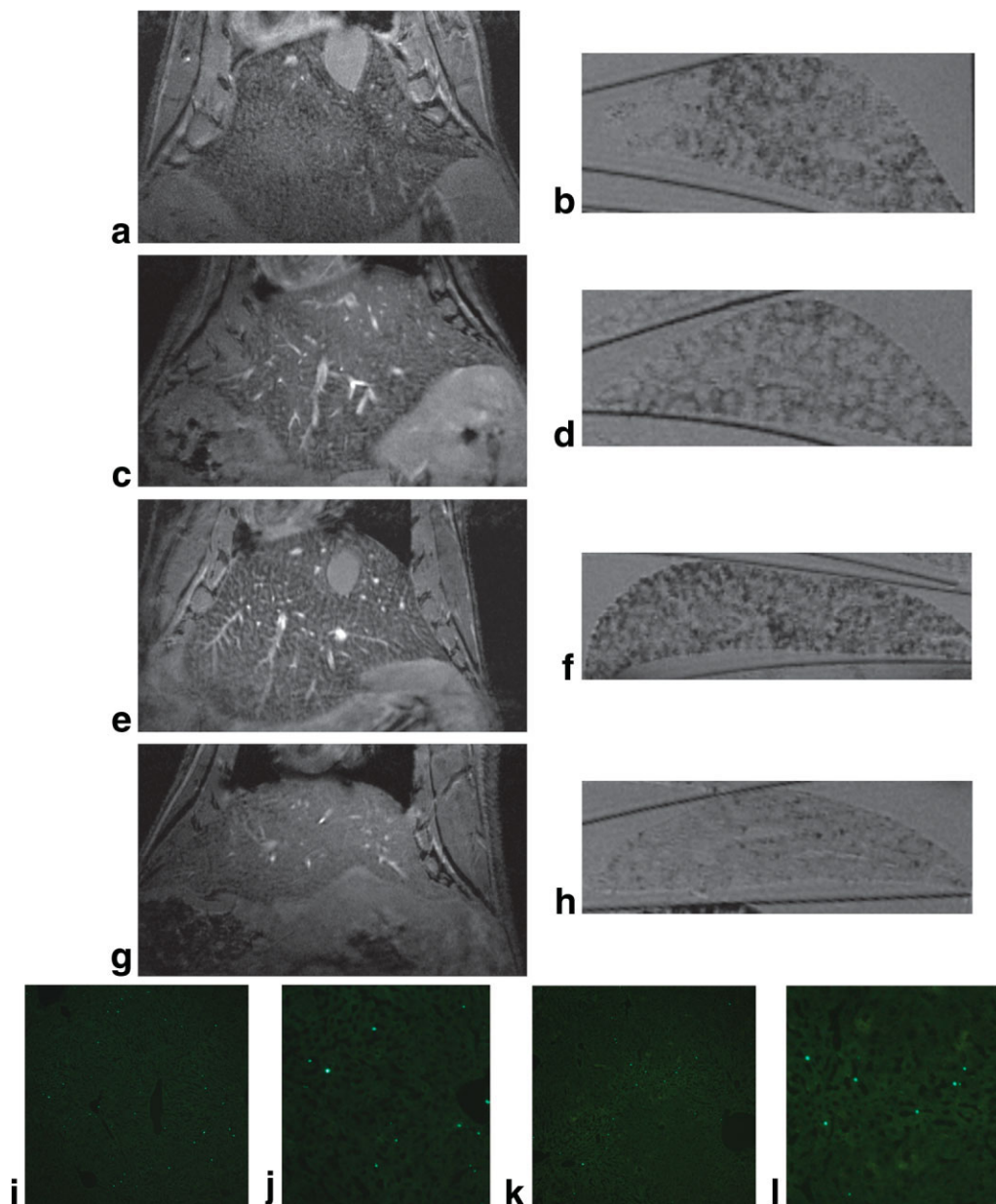


FIG. 4. (a) In vivo and (b) in vitro MRI of the liver from an animal whose spleen was injected with dead labeled cells 1 month prior to MRI. (c) In vivo and (d) in vitro MRI of the liver from an animal whose spleen was injected with free particles only, 1 month prior to MRI. (e) In vivo and (d) in vitro MRI of the liver from an animal that received an i.v. injection of particles. (g) In vivo and (h) in vitro MRI of the liver from an animal whose spleen was injected with live labeled mouse embryonic fibroblasts 1 month prior to MRI. (i) Wide view and (j) expansion of fluorescence stereomicroscopic images of histological sections from the liver in image a, showing only scattered, free particles in the liver. (k) Wide view and (l) expansion of fluorescence stereomicroscopic images of histological sections from the liver shown in c. The wide-view sections are 1.5 mm square, with $3\times$ expansions.

scopy detected mainly scattered individual particles; however, confocal microscopy detected a very few double-labeled cells (data not shown).

To help determine whether the isolated, dark contrast regions were indicative of single cells, an agarose phantom was

constructed that consisted of dispersed single, labeled hepatocytes. The hepatocyte phantom was imaged with imaging parameters mimicking the imaging conditions used to study the liver, both in vivo and in vitro. Figure 5a shows the agarose phantom imaged in the same way as the in vivo

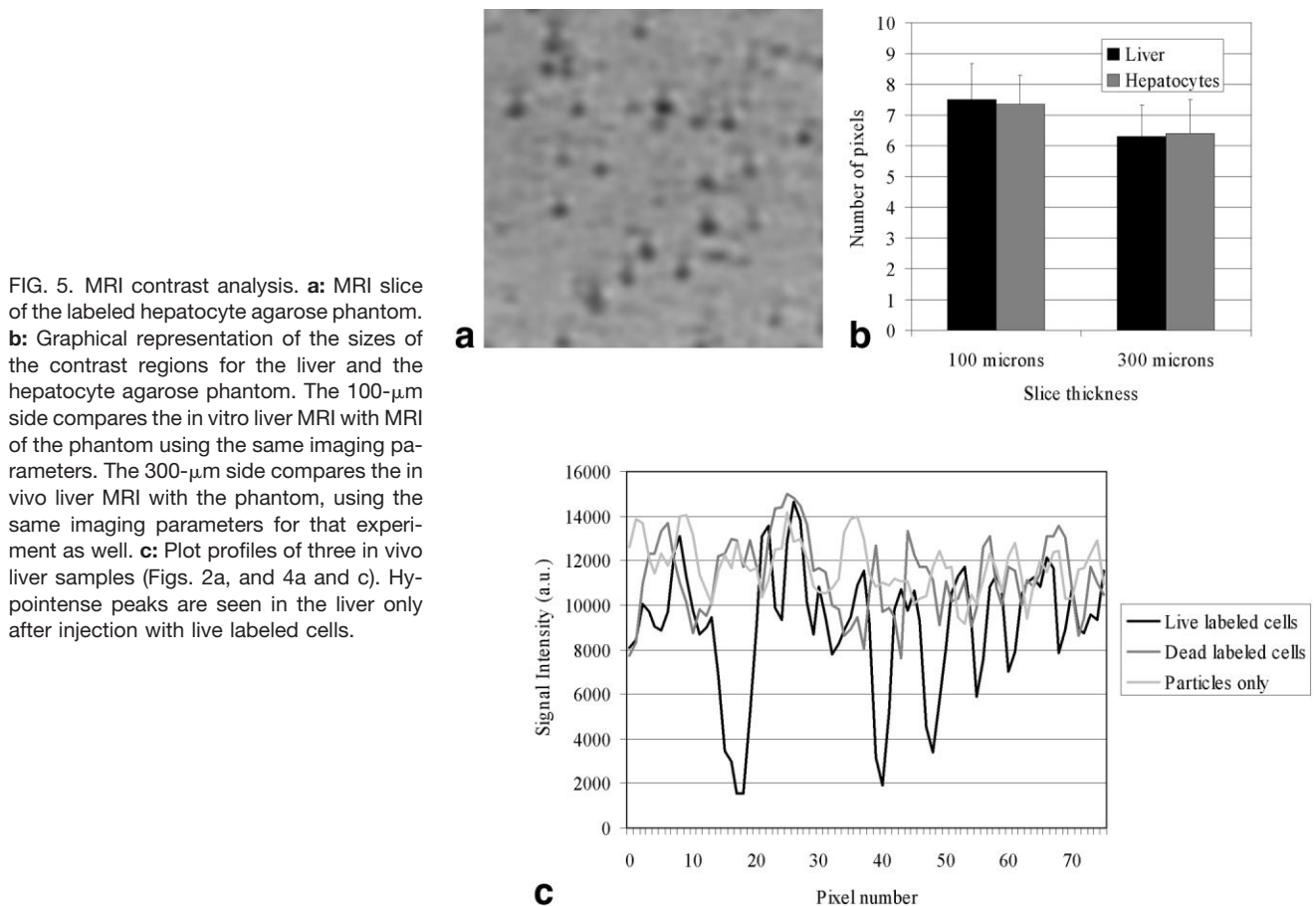


FIG. 5. MRI contrast analysis. **a:** MRI slice of the labeled hepatocyte agarose phantom. **b:** Graphical representation of the sizes of the contrast regions for the liver and the hepatocyte agarose phantom. The 100- μm side compares the in vitro liver MRI with MRI of the phantom using the same imaging parameters. The 300- μm side compares the in vivo liver MRI with the phantom, using the same imaging parameters for that experiment as well. **c:** Plot profiles of three in vivo liver samples (Figs. 2a, and 4a and c). Hypointense peaks are seen in the liver only after injection with live labeled cells.

livers. Isolated, dark contrast regions are observed spotted throughout the sample. Less intense, dark contrast regions are also visible, due to the presence of some remaining free particles in the agarose. The size of seven random dark contrast regions was measured, in both the liver samples and the hepatocyte phantoms, for all imaging conditions (Fig. 5b). The sizes of the contrast regions were nearly identical between the livers and the hepatocytes, regardless of imaging condition. These sizes were 7.50 ± 1.18 and 7.34 ± 0.78 pixels for the in vitro liver and the phantom, respectively, and 6.30 ± 0.95 and 6.40 ± 1.10 pixels for the in vivo liver and the phantom, respectively.

Figure 5c displays line plots through the livers of three different animals (one that received live labeled cells, one that received dead labeled cells, and one that received particles only in the spleen). Only in the liver that received live labeled cells were large hypointense peaks in the signal profile observed. One large hypointense signal around pixel 17 was likely due to several clustered cells; however, the four hypointense peaks at pixels 40, 48, 54, and 59 had signal changes consistent with being caused by single cells. These hypointense signals were 2–3 pixels wide, with signal decreases of 81%, 63%, 45%, and 40%, respectively. The signal profiles of the livers that received dead labeled cells and free particles were similar to each other. The livers exhibited noise-like signal profiles in addition to wide humps of signal intensity. The noise-like signal profiles were a measure of the graininess observed

in the images from these livers, and the wide humps were cross-sections of the circular structures observed.

DISCUSSION

This paper presents the first report of single-cell detection in vivo by MRI following cell labeling and transplantation. In the present study, single-cell detection was made possible by the use of MPIOs for cell labeling, high-resolution MRI, and a well developed cellular migration paradigm that led to relatively isolated cells. MPIOs have been used to efficiently label several different types of cells. The relaxivity of these particles is 50% higher than that of MIONs, based on iron concentration (6). Moreover, the tolerance of these particles by cells is high (>95% survival) because of their inert polymer coating. In this study cells were loaded with >50 pg of iron per cell, as determined by counting particles under confocal fluorescence microscopy, and excellent labeling efficiency was achieved (>90%). Previous studies detected single cells in vitro using MRI (5–8,10,22). Reports of cell detection in vivo have ranged from clusters of a few cells (23) to several hundreds of cells (4). Recent preliminary reports have also been published detailing in vivo single-cell detection by MRI (24,25).

Currently, only two-photon and confocal fluorescence imaging techniques have been used to image single cells noninvasively in vivo. Microscopy is limited by depth of penetration and is confined to only a few hundred microns

within limited FOVs (26). The lower limits for cell tracking by PET, SPECT, and fluorescence imaging techniques have not been determined; however, they will have to overcome poor image resolution (millimeter-sized pixels) to detect single cells in whole animals. MRI is an attractive imaging modality to pursue *in vivo* single-cell detection, for several reasons: it is noninvasive and thus allows longitudinal studies, opaque objects can be imaged with no depth dependence, experiments can be performed in a few hours, it produces excellent background contrast, and three-dimensional acquisitions are possible with voxel sizes approaching cellular dimensions (50 μm).

Because of the difficulty of comparing identical slices of *in vivo* MRI and *in vitro* MRI with histological sections, two lines of evidence are presented to demonstrate that single-labeled cells were observed in the livers of animals that received live labeled hepatocytes. The first was obtained by fluorescence microscopy of the liver histology, including the wide-field and confocal microscopy data. The wide-field data in Fig. 3a show that the spacing between cells in the histology is commensurate to the spacing between cells measured in the MR images of livers (Fig. 2b, e, and f). No attempt was made to directly overlay the MRI data onto the optical data, because of the difficulty of making such comparisons at such high resolution. Our observation of isolated, scattered, clustered groups of particles in the experimental livers, and failure to observe these in the controls indicate that the dark contrast regions in the livers of the experimental animals were due to single cells.

The use of a double-labeling scheme allowed the identification of transplanted cells in the confocal microscope, as opposed to endogenous cells of the host that may have picked up the contrast agent following cell death. We assumed that if the cells had died, the red cell tracker and green fluorescent MPIOs would have been diluted. Genetic markers, such as green fluorescent protein (GFP) (4) and beta-galactosidase (27), have also been used as fluorescent labels for cell transplantation studies. Following cell transplantation, cells can either survive or die, and if they survive the question arises as to whether they grafted in the spleen or the liver. The mechanisms and routes of engraftment for transplanted cells were previously elucidated (19). Additionally, it is known that as many as 85% of transplanted cells die (Dr. Ira Fox, M.D., University of Nebraska Medical Center, personal communication). Only if the transplanted cells migrated to the liver, carrying both particles and cell tracker dye, would both red and green fluorescence colocalize within a cell under the microscope. Additionally, based on the measurements in Fig. 5a of contrast region size for a single, labeled hepatocyte, the dark, discreet contrast in the livers that received live labeled cells could only be due to grafted hepatocytes. If the cells had grafted only to the spleen and survived, the liver would have had no contrast because there would have been no particles in the liver.

Conversely, if the cells die during transplantation, the question arises as to when and where they died. In this case, the considerations were whether the cells died in the liver or the spleen, and what was the fate of the contrast agent. If the cells died in the spleen, particles could have become free and could either have remained in the spleen or traveled to the liver, where they would have been endocytosed by the mac-

rophages of the liver, the Kupffer cells. These scenarios were tested with two controls: 1) injection of dead, labeled hepatocytes, and 2) injection of free particles into the spleen. If the cells died in the liver, then again the particles would have become free and would have been endocytosed by Kupffer cells, as well as host hepatocytes. This scenario was difficult to control for, since injecting dead hepatocytes into the liver would not have dispersed them throughout the liver, and the cells would not have been isolated enough for us to detect individuals. In all cases, the only fluorescence detectable would have been the green fluorescence from the particle, and not the red fluorescence from the cell tracker. This was consistently observed in the fluorescence microscopy results (shown in Fig. 4i–l). Additionally, the MRI contrast would have reflected that of dispersed single or few particles spread out throughout the tissue. This contrast would have appeared grainy and less intense than isolated groups of cells containing many packed particles, exactly as shown in the MR images of the control livers in Fig. 4a–h. Additionally, this contrast would have been confined largely to the periphery of liver lobules, close to the arterial input to the liver, since resident macrophages in these areas would be the first to contact these particles and endocytose them. The circular shapes of dark contrast observed in the MR images (Fig. 4a–h) of control livers in which dead cells and free particles were injected into the animals were probably due to the outlines of the liver lobules.

The second major line of evidence indicating that the dark contrast regions were due to single cells resulted from the comparison of the sizes and hypointensities of the dark contrast spots observed *in vivo* and *in vitro* in the liver with those of labeled hepatocytes in an agarose phantom. Nearly identical sizes of contrast regions were observed in identical imaging conditions (roughly 6.4 and 7.4 pixels for 100 μm (*in vitro* comparison) and 300 μm slice thickness (*in vivo* comparison), respectively). The sizes of these contrast regions matched those previously observed for isolated labeled hepatocytes grown on culture dishes (10). Interestingly, the contrast in the images obtained using thicker slices was $\sim 20\%$ greater than achieved with thinner slices. This was likely because the spatial extent of the effect of iron oxide is not symmetrical, but rather has a complex pattern (28). It may be that a thicker slice captured all of the contrast from a labeled hepatocyte better than a thinner slice, because all of the effects of the iron oxide contrast were included in the voxel. Additionally, the wider slice thickness protocol used a slice-selective 2D gradient-echo scheme, and this slice-select pulse may have enhanced the size of the contrast region by failing to excite water molecules in the vicinity of the contrast agent. The water in this case is within the static dephasing regime (29,30) and is likely shifted from the nominal resonance frequency of water.

The MRI parameters used (specifically the gradient-echo time and image resolution) were important factors in detecting single cells in liver. Since the dominant contrast mechanism is susceptibility-based dephasing of water near the particles, gradient-echo MRI is best suited for this purpose. However, the liver has a short background T_2^* , and thus lengthy TEs would result in total signal loss from the liver. In an earlier study, imaging conditions (including gradient-echo time and image resolution) were established for visualizing single

cells in different tissues (10). It was shown that image resolution should be 100 μm isotropic or better for robust detection of single cells when using TEs of 3–5 ms. The TE used in these experiments was 4 ms. The image resolution (100 \times 100 \times 300 μm) was chosen to be close to those recommendations, yet allow for more rapid imaging. Individual 1.63- μm MPIOs can be robustly visualized at 100 μm or higher resolution (7), so the 300- μm slice thickness helped to minimize images of contrast from isolated free particles. While particles as large as 5.80 μm have been used to label cells, because of their robust detection at 200–300 μm resolution, it would have been difficult to distinguish between cells and free particles with MRI. Livers with a lot of free particles still showed significant contrast; however, Fig. 5c shows that the contrast was less hypointense than that in a well-labeled cell with many clustered particles, and was easily distinguishable. Now that it is possible to detect individual cells, it will be critical to develop robust strategies to distinguish single cells from clusters of cells, or contrast agent that leaked from dead cells.

CONCLUSIONS

In conclusion, single hepatocytes labeled with 1.63- μm MPIOs can be detected in the liver following transplantation into the spleen. The use of heavily labeled cells (>50 pg iron) enabled engrafting cells to be separated from free particles, which may have been taken up by the liver due to cell death. This should enable the development of rapid-assay strategies to increase the efficiency of engraftment of liver cell transplants. In addition, it should be possible to detect single cells in other tissues using MPIO-labeled cells.

ACKNOWLEDGMENTS

The authors thank Dr. Ira Fox of the Department of Surgery, University of Nebraska Medical Center, for helpful discussions. Dr. Carolyn L. Smith of the NINDS Light Imaging Facility is acknowledged for her assistance in acquiring the confocal fluorescence images.

REFERENCES

- Hill JM, Dick AJ, Raman VK, Thompson RB, Yu ZX, Hinds KA, et al. Serial cardiac magnetic resonance imaging of injected mesenchymal stem cells. *Circulation* 2003;108:1009–1014.
- Zhang Y, Dodd SJ, Hendrich KS, Williams M, Ho C. Magnetic resonance imaging detection of rat renal transplant rejection by monitoring macrophage infiltration. *Kidney Int* 2000;58:1300–1310.
- Anderson SA, Glod J, Arbab AS, Noel M, Ashari P, Fine HA, Frank JA. Noninvasive MR imaging of magnetically labeled stem cells to directly identify neovasculature in a glioma model. *Blood* 2005;105:420–425.
- Hoehn M, Kustermann E, Blunk J, Wiedermann D, Trapp T, Wecker S, Focking M, Arnold H, Hescheler J, Fleischmann BK, Schwindt W, Buhrl C. Monitoring of implanted stem cell migration in vivo: a highly resolved in vivo magnetic resonance imaging investigation of experimental stroke in rat. *Proc Natl Acad Sci USA* 2002;99:16267–16272.
- Dodd SJ, Williams M, Suhan JP, Williams DS, Koretsky AP, Ho C. Detection of single mammalian cells by high-resolution magnetic resonance imaging. *Biophys J* 1999;76:103–109.
- Hinds KA, Hill JM, Shapiro EM, Laukkanen MO, Silva AC, Combs CA, Varney TR, Balaban RS, Koretsky AP, Dunbar CE. Highly efficient endosomal labeling of progenitor and stem cells with large magnetic particles allows magnetic resonance imaging of single cells. *Blood* 2003;102:867–872.
- Shapiro EM, Skrtic S, Sharer K, Hill JM, Dunbar CE, Koretsky AP. MRI detection of single particles for cellular imaging. *Proc Natl Acad Sci USA* 2004;101:10901–10906.
- Foster-Gareau P, Heyn C, Alejski A, Rutt BK. Imaging single mammalian cells with a 1.5 T clinical MRI scanner. *Magn Reson Med* 2003;49:968–971.
- Renshaw PF, Owen CS, Evans AE, Leigh Jr JS. Immunospecific NMR contrast agents. *Magn Reson Imaging* 1986;4:351–357.
- Shapiro EM, Skrtic S, Koretsky AP. Sizing it up: cellular MRI using micron-sized iron oxide particles. *Magn Reson Med* 2005;53:329–338.
- Frank JA, Miller BR, Arbab AS, Zywicke HA, Jordan EK, Lewis BK, Bryant LH, Jr, Bulte JW. Clinically applicable labeling of mammalian and stem cells by combining superparamagnetic iron oxides and transfection agents. *Radiology* 2003;228:480–487.
- Moore A, Basilion JP, Chioocca EA, Weissleder R. Measuring transferrin receptor gene expression by NMR imaging. *Biochim Biophys Acta* 1998;1402:239–249.
- Ahrens ET, Feili-Hariri M, Xu H, Genove G, Morel PA. Receptor-mediated endocytosis of iron-oxide particles provides efficient labeling of dendritic cells for in vivo MR imaging. *Magn Reson Med* 2003;49:1006–1013.
- Bulte JW, Zhang S, van Gelderen P, Herynek V, Jordan EK, Duncan ID, Frank JA. Neurotransplantation of magnetically labeled oligodendrocyte progenitors: magnetic resonance tracking of cell migration and myelination. *Proc Natl Acad Sci USA* 1999;96:15256–15261.
- Zhao M, Kircher MF, Josephson L, Weissleder R. Differential conjugation of tat peptide to superparamagnetic nanoparticles and its effect on cellular uptake. *Bioconjug Chem* 2002;13:840–844.
- Pirko I, Johnson A, Ciric B, Gamez J, Macura SI, Pease LR, Rodriguez M. In vivo magnetic resonance imaging of immune cells in the central nervous system with superparamagnetic antibodies. *FASEB J* 2004;18:179–182.
- Shapiro EM, Skrtic S, Koretsky AP. Long term cellular MR imaging using micron sized iron oxide particles. In: Proceedings of the 12th Annual Meeting of ISMRM, Kyoto, Japan, 2004. Abstract 1734.
- Gupta S, Chowdhury JR. Therapeutic potential of hepatocyte transplantation. *Semin Cell Dev Biol* 2002;13:439–446.
- Fox JJ, Chowdhury JR. Hepatocyte transplantation. *Am J Transplant* 2004;6:7–13.
- Ponder KP, Gupta S, Leland F, Darlington G, Finegold M, DeMayo J, Ledley FD, Chowdhury JR, Woo SL. Mouse hepatocytes migrate to liver parenchyma and function indefinitely after intrasplenic transplantation. *Proc Natl Acad Sci USA* 1991;88:1217–1221.
- Seglen PO. Hepatocyte suspensions and cultures as tools in experimental carcinogenesis. *J Toxicol Environ Health* 1979;5:551–560.
- Lewin M, Carlesso N, Tung CH, Tang XW, Cory D, Scadden DT, Weissleder R. Tat peptide-derivatized magnetic nanoparticles allow in vivo tracking and recovery of progenitor cells. *Nat Biotechnol* 2000;18:410–414.
- Kircher MF, Allport JR, Graves EE, Love V, Josephson L, Lichtman AH, Weissleder R. In vivo high resolution three-dimensional imaging of antigen-specific cytotoxic T-lymphocyte trafficking to tumors. *Cancer Res* 2003;63:6838–6846.
- Wu YL, Foley L, Hitches TK, Williams JB, Ye Q, Ho C. Non-invasive in vivo “histology”: visualizing single immune cells in acute allograft rejection after heterotropic heart transplantation with micrometer-sized iron oxide containing particles. *J Cardiovasc Magn Reson* 2005;7:7–8.
- Heyn C, Ronald JA, MacKenzie L, Chambers AF, Rutt BK, Foster PJ. MRI of single SPIO labeled cells in mice on a 1.5T clinical scanner. In: Proceedings of the 13th Annual Meeting of ISMRM, Miami Beach, FL, USA 2005. Abstract 2624.
- Gao X, Cui Y, Levenson RM, Chung LW, Nie S. In vivo cancer targeting and imaging with semiconductor quantum dots. *Nat Biotechnol* 2004;22:969–976.
- Walter GA, Cahill KS, Huard J, Feng H, Douglas T, Sweeney HL, Bulte JW. Noninvasive monitoring of stem cell transfer for muscle disorders. *Magn Reson Med* 2004;51:273–277.
- Callaghan PT. Principles of nuclear magnetic resonance microscopy. Oxford, England: Clarendon Press; 1993.
- Bowen CV, Zhang X, Saab G, Gareau PJ, Rutt BK. Application of the static dephasing regime theory to superparamagnetic iron-oxide loaded cells. *Magn Reson Med* 2002;48:52–61.
- Yablonskiy DA, Haacke EM. Theory of NMR signal behavior in magnetically inhomogeneous tissues: the static dephasing regime. *Magn Reson Med* 1994;32:749–763.